OPTIMIZING WING SAIL EFFICIENCY: A COMPUTATIONAL FLUID DYNAMIC APPROACH TO UNDERSTAND STALL RECOVERY

A.M. Wright, L.E Jones & M.P. Prince Wolfson Unit M.T.I.A., University of Southampton, UK

SUMMARY

This paper presents a computationally based approach for modelling stall recovery, using an idealisation of a current design of a single multi-element wing in isolation to investigate the effect of wing realignment in different scenarios, from which a control algorithm can be derived. The wing and ship were simulated using unsteady RANS, utilising a dynamic mesh to capture the wing motion. Validation of the process is presented using available wind tunnel data, followed by an example case study, highlighting stall hysteresis. The magnitude of loss of drive for different wing movements are presented alongside recorded masthead flow velocity and surface pressure from which the design of both performance monitoring and wing control mechanisms can be investigated and developed.

NOMENCLATURE

υ Kinematic viscosity (N s m⁻²)

ρ Density (kg m⁻³)
 A Plan area of wing (m²)
 AWA Apparent Wind Angle (deg)
 AWS Apparent Wind Speed (m/s)
 AoA Angle of Attack (deg)

D Drag (N)

F_{DRIVE} Drive Force (N); force in direction of vessels centreline

L Lift (N)
P Pressure (N/m²)
TWA True Wind Angle (deg)
U Freestream velocity (m/s)

 $\begin{array}{ll} C_{DRAG} & Coefficient of drag = D/(\frac{1}{2} \rho AU^2) \\ C_{DRIVE} & Coefficient of drive = F_{DRIVE}/(\frac{1}{2} \rho AU^2) \\ C_{LIFT} & Coefficient of lift = L/(\frac{1}{2} \rho AU^2) \\ C_{P} & Coefficient of pressure = P/(\frac{1}{2} \rho U^2) \\ \end{array}$

1. INTRODUCTION

The principal performance metric of commercial vessels (in contrast to many sailing yacht studies) is cost. That is the need to transport the cargo as efficiently as possible in terms of financial cost and within particular time schedules. Commercial shipping operators have always been aware of wind propulsion, but wind fell out of favour with the lower costs and increased reliability of engines. The balance is now swinging back towards wind propulsion with the requirement for decarbonization, primarily via the imposition of IMO's Greenhouse Gas Strategy and the Energy Efficiency Existing Ship Index (EEXI) technical measures, which raises the topic which is the final arbitrator: money, and more specifically capital and operational expenditure. While it is expected that capital expenditure will be higher due to installation of both an engine and additional propulsion system, the voyaging costs, and hence total operational costs, will be lower due to lower energy use. However, "there is a lack of sufficient performance data for both discussed technologies" [1]. This is not unusual with a "new" technology that is embryonic and expensive; over time it becomes cheaper as production and thus efficiencies of scale increase.

There are currently a variety of different wind assisted shipping concepts, all with their own proponents, at various different stages of technical development and real-world implementation [2]. One such approach is the use of rigid wing sails, made of a number of elements, attached to the deck of the vessel and arranged such that drive force is generated from the air flow over the passive surface. A number of such devices have been in use on commercial ships in the last two years (BAR Technologies "windwing" for example) and there are a number of other near market alternatives such as AYRO "Oceanwings", Michelin "Wisamo" and Smart Green Shipping "Fastrig" to name a few.

For a wide range of conditions, optimising drive from wing sails requires operating close to peak lift. This results in increased chance of stall occurring with small perturbations in the environmental conditions (wind shift, change in wind speed, vessel movement, etc.). If the wing is not realigned the flow can easily stay stalled even after the initial conditions are regained, thus greatly lowering drive and overall system efficiency. A well refined control system will quickly identify stall, change the angle of incidence to re-attach flow and then move back to peak drive force and system efficiency.

This study provides an approach to assess the sensitivity of various single and multi-element wing systems to stall in unsteady conditions and allows various control strategies to be tested at the design stage. Without a full understanding of stall characteristics and behaviour optimal performance cannot be designed for nor maintained due to a range of possibilities, such as sudden and sharp loss of lift, the wing remaining stalled after a change in the conditions or reduced drive due to an overly conservative angle of attack being used.

3. COMPUTATIONAL FLUID DYNAMICS METHODOLOGY

Computational Fluid Dynamic (CFD) simulations were conducted on the IRIDIS 6 high performance computing cluster at the University of Southampton using the OpenFOAM toolbox, with details as follows:

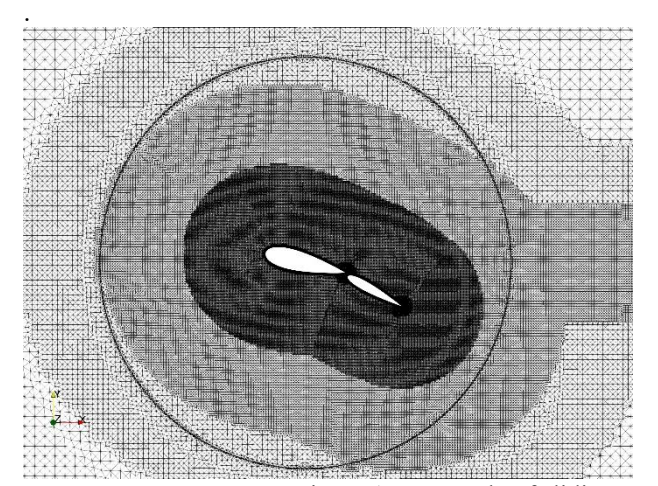
- Simulations were conducted using an unsteady Reynolds averaged Navier-Stokes (URANS) based transient solver.
- The wing was modelled as rotating by specifying a sliding mesh.
- Simulations were conducted at 1:1 scale, hence at full-scale Reynolds numbers (up to $7x10^5$ for the wind tunnel validation data and $7x10^6$ for the case study wing)
- The air was assumed to be 15 degrees Celsius.
- Turbulence effects were accounted for using a kappa-omega SST turbulence model, with the viscous sublayer modelled using wall functions.

The simulations are comparatively expensive in computational terms due to the use of moving meshes and the requirement to model temporal effects of wing movement.

3.1 MODELLING OF MOVING SURFACES

For a non-articulating wing, the effects of a change in angle of attack to the incoming air flow can nominally be modelled by either rotating the geometry or by rotating the inflow. The inclusion of dynamic meshing required by geometry movement is more computationally expensive than just rotating the inflow angle, but altering the inflow angle does not allow detailed control of the flow the foil observes due to numerical damping and diffusion of the flow between the boundary and the wing geometry, which can be a significant distance if the whole vessel is incorporated into the simulation.

The inclusion of relative motion between the elements of the wing and the desire to model the wing responding to a change in the inflow wind requires modelling of changes in the geometry position and orientation, which is achieved by various Arbitrary Mesh Interface (AMI) modelling approaches. In cases where only the overall angle of attack is altered then a sliding mesh is utilised where an inner zone of the domain, containing the wing, rotates within the other (i.e. outer) domain, with the cells non overlapping. When flap movement relative to the main wing is incorporated into the model then an overlapping mesh is required, due to the flap centre of rotation overlapping with the main foil element. All results presented in this paper are for fixed flap angle, and hence using only the sliding mesh approach, with an example of the meshing shown in Figure 1.



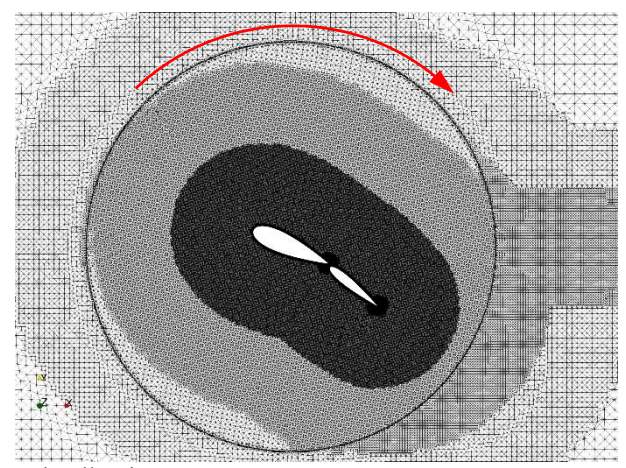


Figure 1 – Example of sliding AMI mesh, allowing geometry to rotate

3.2 DOMAIN AND BOUNDARY SPECIFICATION

The vessel centreline is aligned with the Y=0 plane, and the inflow velocity is rotated to provide the desired true wind direction. This allows the creation and maintenance of a twisted flow boundary condition, created from the superposition of vessel speed and atmospheric boundary layer wind speed. The initial wing sail and flap rotation relative to the vessel is applied as a rotation of the geometry prior to simulation. Thus the vessels longitudinal plane is in the X direction, transverse plane is in the Y direction and vertical is in the Z direction.

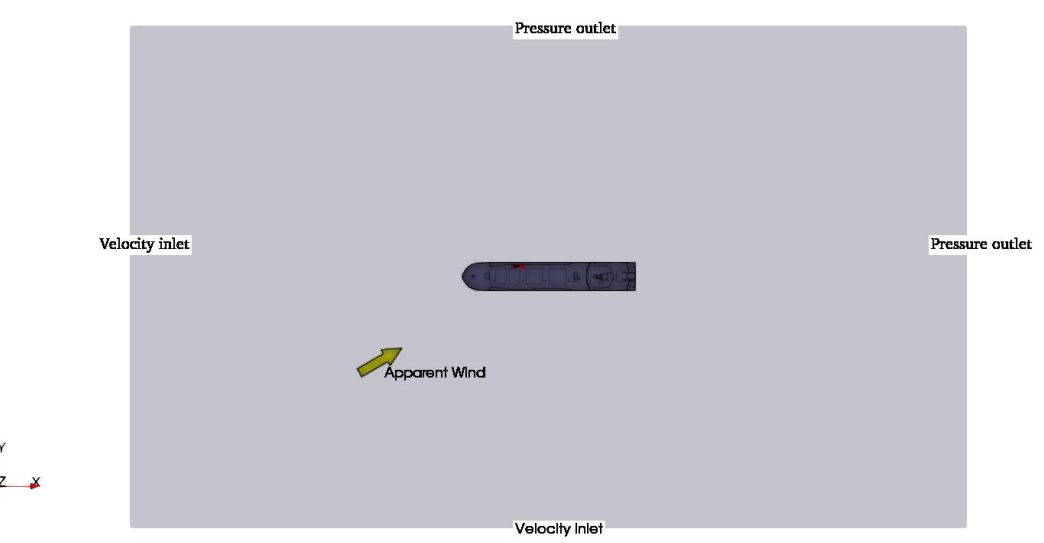


Figure 2 – Computational domain orientation and boundary conditions

The overall domain was sufficiently large to ensure no pressure gradient at the boundaries, which allowed the velocity to be set on two upstream faces and the pressure at the two downstream outlets, as shown in Figure 2. A symmetry plane was placed at an appropriate distance above the vessel and the sea surface is defined as a moving wall boundary.

It has been found from previous unpublished case studies that maintaining the vessel orientation and rotating the inflow velocity, rather than maintaining the inflow mean direction and rotating the vessel, is more accurate and more computationally efficient due to the cross domain velocities generated by the twisted flow boundary condition creating a transverse pressure gradient.

4. VERIFICATION OF COMPUTATIONAL MODEL

To validate the approach, for both static and dynamic effects, the wind tunnel test data presented by Hillenbrand et all [3] was used. The data presented is for a two element wing, 'Oceanwing', 1m tall and aspect ratio of 2.86, tested at the L2000 flight-dynamics wind tunnel at KTH Royal Institute of Technology in Stockholm, Sweden.

A detailed series of tests were conducted, varying limits of motion and flap angles, from which a selection of 15° flap cases have been modelled. The wind tunnel data has two sets of data -

- Flap angle 15°, angle of attack increases to 30° and then decreases at a rate of 0.5°/s
- Flap angle 15°, angle of attack increases to 20° and then decreases at a rate of 0.5°/s

There are three sets of CFD simulations data conducted for this study -

- steady state at a specific angle of attack
- transient, starting at 14° angle of attack and increasing at 0.5°/s
- transient, starting at 25° angle of attack and decreasing at 0.5°/s

For these cases the inclusion of vessel speed and atmospheric boundary layer are not present and hence the boundary conditions are a trivial version of the model, with constant speed and direction.

A base mesh dependency study was conducted for a typical case (14° angle of attack with 15° flap), reviewing both domain size and mesh density. Figure 3 present the variation in lift and drag for different mesh densities, where forces for a given solution are presented as a ratio of the force for the highest density mesh (Lo and Do), which is assumed to be mesh independent. All further steady state solutions were conducted with approximately 80M cells.

The lift and drag from steady state and transient CFD simulations is presented in Figures 4 and 5, alongside the wind tunnel data.

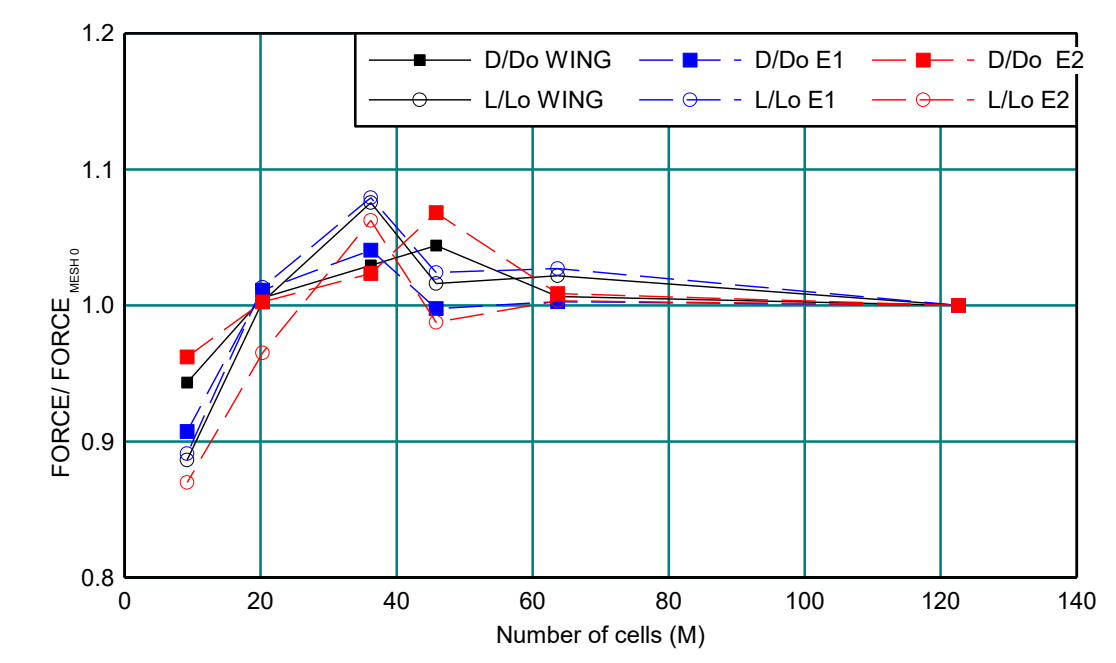


Figure 3 - Variation in lift and drag from Oceanbird wing with mesh density

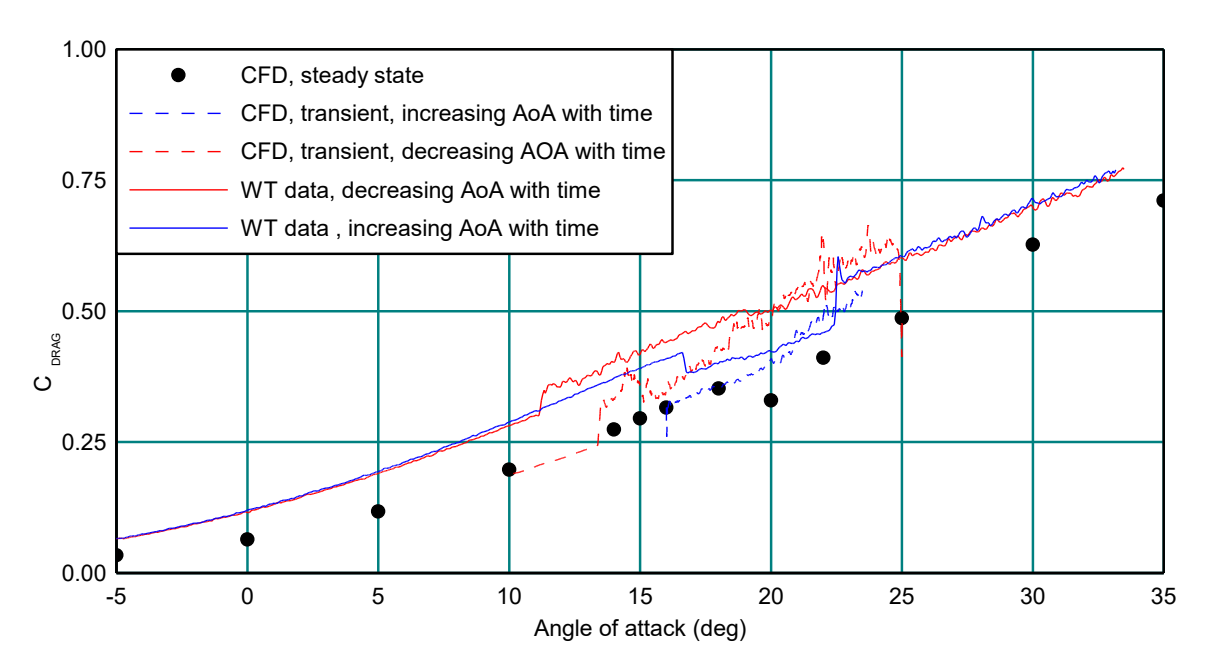


Figure 4 - Variation in drag coefficient for Oceanbird wing against angle of attack

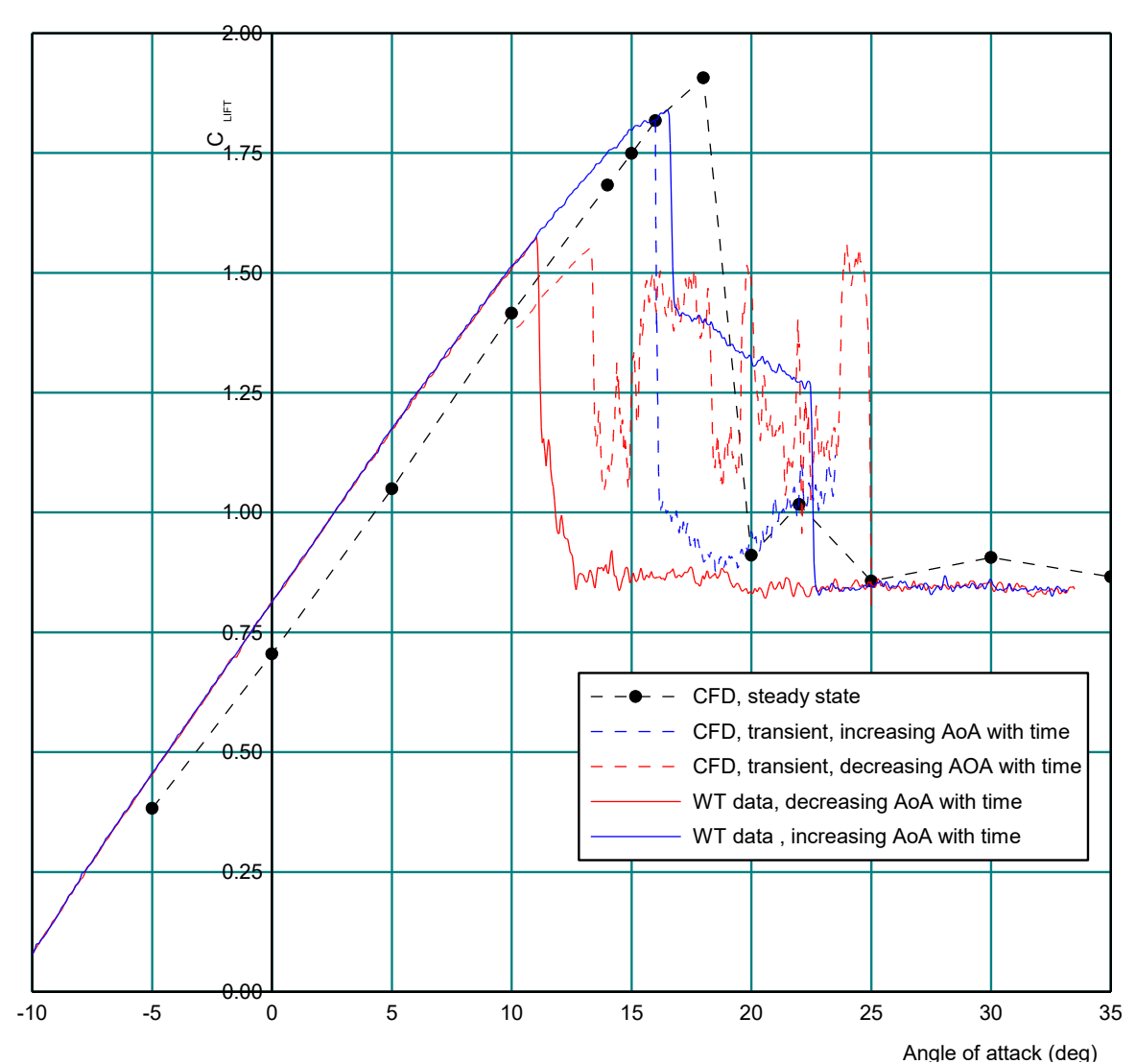


Figure 5 – Variation in lift coefficient for Oceanbird wing against angle of attack

Overall the data shows good correlation to the wind tunnel data, principally until stall. The peak lift, lift curve slope and fully stalled drag and lift values are all very close, and the lift in the region of stall shows sections of CFD simulation data with the same initial stall lift. There is however an approximate 1° offset in lift and the CFD data shows greater unsteady loading in the region of stall.

It is noted that the wind tunnel data was undertaken at a Reynolds number of 700 000, a regime where significant regions of laminar flow may be expected, however turbulence stimulation was not employed to produce in the experimental test data presented. Due to the Reynolds number regime and lack of turbulence stimulation, the dynamic separation and reattachment behaviour may be strongly impacted by regions of laminar flow. In addition, the data has been presented without any corrections due to the presence of the wind tunnel walls.

It is to be expected that wall correction and wake blockage corrections will alter the inflow angle by up to 1.5°, and blockage corrections, particularly near stall where a large wake is present, will cause the drag and lift values to drop by a few percent. The Reynolds number of the wing means the results are very sensitive to small perturbations or alterations in flow condition, both in the wind tunnel data and the CFD modelling, and an increased level of uncertainty can be expected to the data. In light of these uncertainties, the CFD method is considered able to model the behaviour observed experimentally acceptably.

5. CASE STUDY GEOMETRY

The solid wing sail used as a case study is based on an existing 20m span solid wing sail. Figure 6 shows the overall dimensions. It is a two element wing with the second element consisting of four segments, all mounted upon a 4m tall base containing hydraulics and other systems.

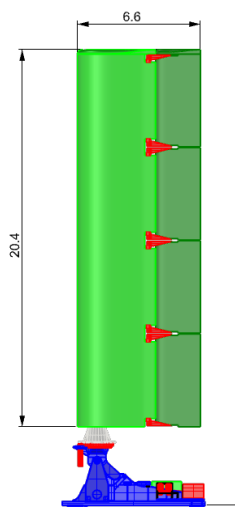


Figure 6 – Case study wing sail dimensions

6. MODELLING OF CASE STUDY RIG

A similar approach to the Oceanbird wing (verification case, §4) was taken for the case study geometry, with the domain size increasing in accordance with the wing size (to dimensions 50m by 25m by 30m) and the only critical difference being the use of two velocity inlets, leaving the nominal vessel centreline on the Y=0 plane, as described in section 3.2.

The cases considered are the wing operating close to peak efficiency (i.e. maximum drive force), which is then subjected to a wind shift causing the wing to stall. Two scenarios are considered:

- Scenario 1: A boat speed of 10 knots with a true wind speed of 20 knots at an angle of 30.0° from the bow, giving at AWA of 20.1° and AWS of 29 knots (14.55m/s) subjected to a 10° change in apparent wind direction
- Scenario 2: A boat speed of 10 knots with a true wind speed of 20 knots at an angle of 60.0° from the bow, giving an AWA of 40.89° and AWS of 26.5 knots (13.61m/s) which is subjected to a 10° shift in true wind direction.

The second scenario is a more authentic case, with higher drive and a more realistic change in conditions, but the first case is presented to highlight the different effects in play, in addition to the basic aerodynamic phenomenon of stall. For the 30° TWA case the wing is initially set at an angle of -10° to the nominal centreline giving an angle of attack of 10° to the free-stream wind, while the 60° TWA case has the wing set initially at -28° to the centreline giving an angle of attack of 13° . In both cases the flap angle was 20° .

The wing has to respond to the change in wind direction to regain optimal drive and different hypothetical speeds of response are assessed. The cases modelled for the $TWA=30^{\circ}$ scenario were—

- No wind shift and no wing movement
- Apparent wind shift of 10°, no wing movement
- Apparent wind shift of 10°, wing responds at 2.5°/s
- Apparent wind shift of 10°, wing responds at 0.5°/s

For the TWA=60° scenario, the cases modelled were -

- Apparent wind shift of 10°, no wing movement
- Apparent wind shift of 10° , wing responds at $4^{\circ}/s$
- Apparent wind shift of 10°, wing responds at 0.5°/s

The wind shift was implemented by an enforced change in the flow speed at the boundary (40m upstream of the wing). For the TWA=30° scenario, at 5 seconds the wind shifts direction by 10 degrees, then rotates back to the original angle after 5 seconds at the new direction. The magnitude of the wind speed was not changed. For the TWA=60° scenario the true wind shifts direction by 10 degrees at 5 seconds, then rotates back to the original angle after 10 seconds at the new direction which causes an increase in the apparent wind angle and a drop in the apparent wind speed.

7. MONITORING OF STALL AND OPTIMAL WING ORIENTATION

There are various approaches to monitoring local conditions around the wing, usually one of –

- Forces generated by wing typically recorded via strain gauges on the main slew ring
- Inflow wind speed and angle recorded via an anemometer placed above the wing
- Pressure on surface of wing recorded via pressure tappings on the wing surface

Of these three approaches, force monitoring gives little information as to what has occurred, other than drive and side force have changed, and vessel motion will induce inertial loading causing a more complex control algorithm. A mast head anemometer will most likely by in use anyway for general weather observations and initial wing control, while pressure tappings will give the most information as to the flow over the wing but require additional systems and monitoring.

The use of local apparent wind angle combined with a knowledge of the wings aerodynamic performance is, in general, enough to maintain the wing at optimal angle of attack. Different atmospheric conditions (turbulence levels, wind profile etc) as well as changes to vessel layout will however alter the wings performance for a specific wind speed and direction at the mast head. In addition, the presence of the wing with the associated tip vortex can have a complex upwash influence upon the recorded wind speed and angle. Pressure tappings give more detailed information, such as the level of separated flow, and an indirect measure of the forces at as many locations as are monitored, thus greater knowledge and more information to feed into the control algorithm. The downside of pressure tappings is more instrumentation, data logging and processing before importing to the control system.

For this study the local apparent wind has been used in order to keep the control concept simple and minimise the variables, allowing a simple lookup table of current apparent wind angle against optimal angle of attack for generating drive force. The wing response was triggered by monitoring of the masthead apparent wind angle; when a change of more than 4 degrees was recorded for more than 2 seconds, then the rig was rotated to re-gain the optimal angle of attack. Note that this angle may not be the same as the original angle of attack, depending upon the current apparent wind angle. For small apparent wind angles L/D efficiency is critical but as the AWA increases towards 90° then the optimal angle changes towards one of maximum lift.

8. CASE STUDY RESULTS

8.1 30° TWA CASE

In addition to recording forces generated by the wing, velocity and pressure probe points have been placed above the tip of the wing (2m forward of the rotation point, and 2m above the tip) and at regular intervals around the mid span wing surface, simulating a mast head anemometer and surface pressure tappings respectively. Figure 7 presents the wind speed recorded above the wing for the cases modelled, while Figure 8 presents the pressure at four points on the suction side of the wing. Slices throught the solution are shown in Figure 9 for the cases where the wing doesn't respond and responds at 2.5°/s and the resultant forces generated for the different cases modelled are presented in Figure 10.

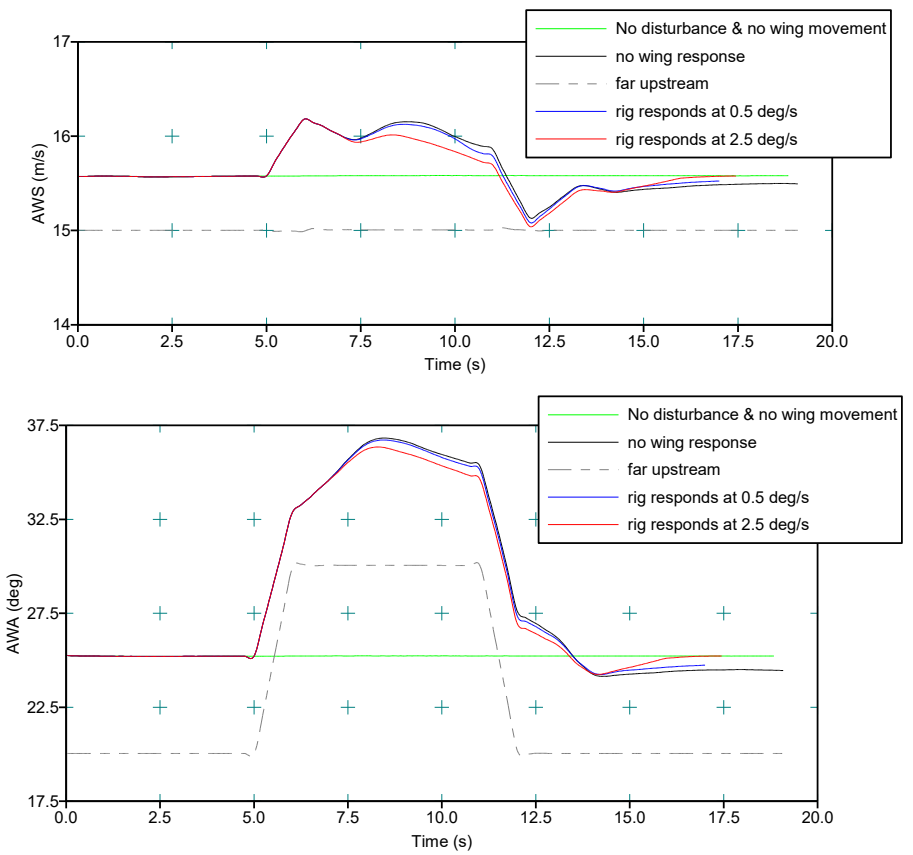


Figure 7 – Apparent wind recorded above wing, TWA 30°

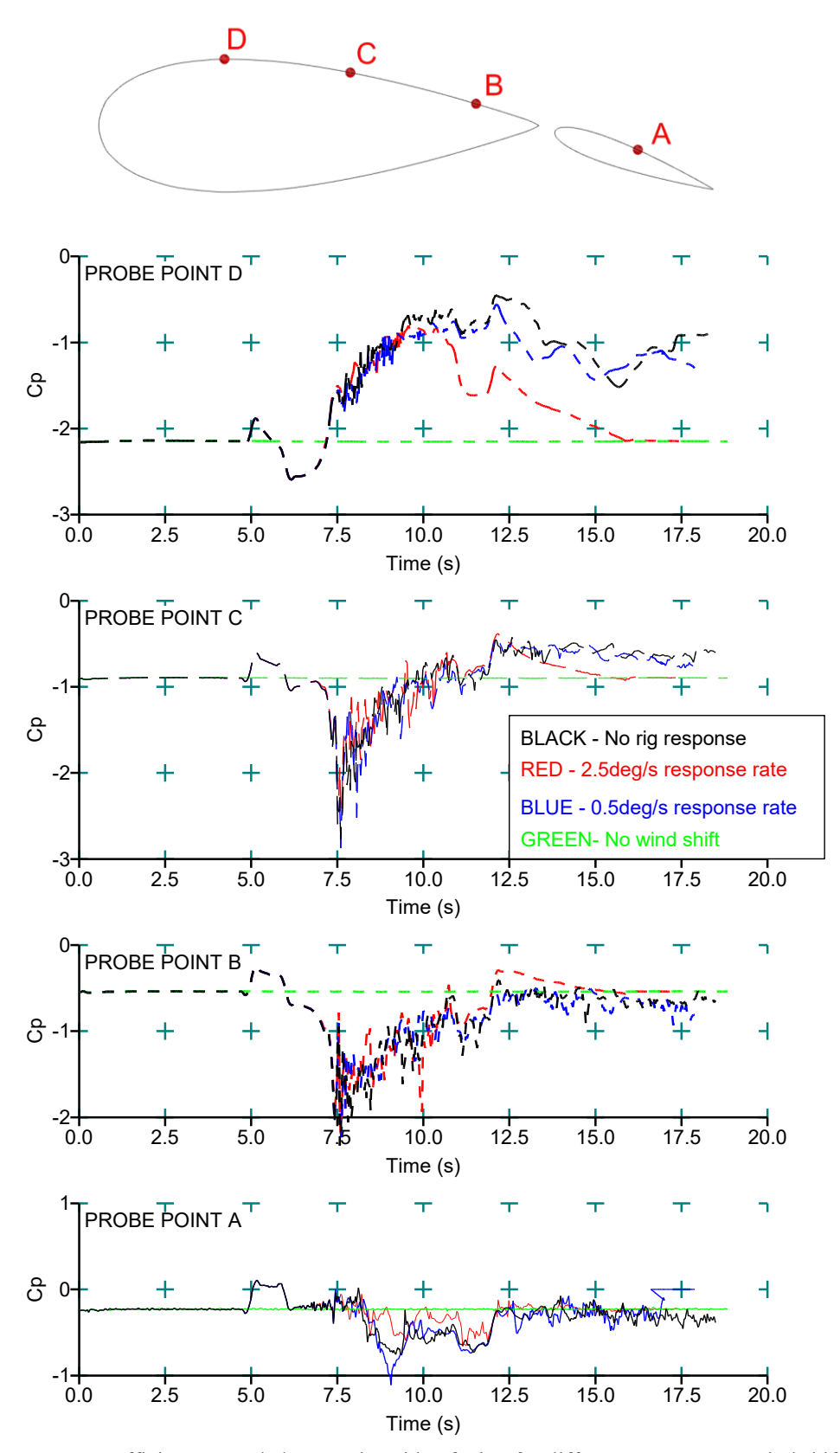
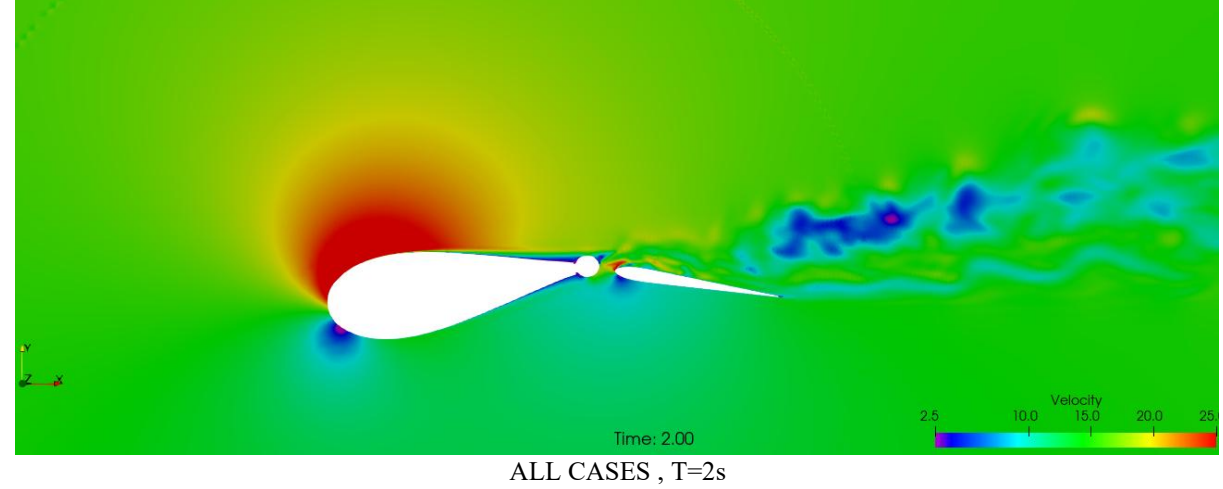


Figure 8 - Pressure coefficients recorded on suction side of wing for different responses to wind shift, TWA 30°line



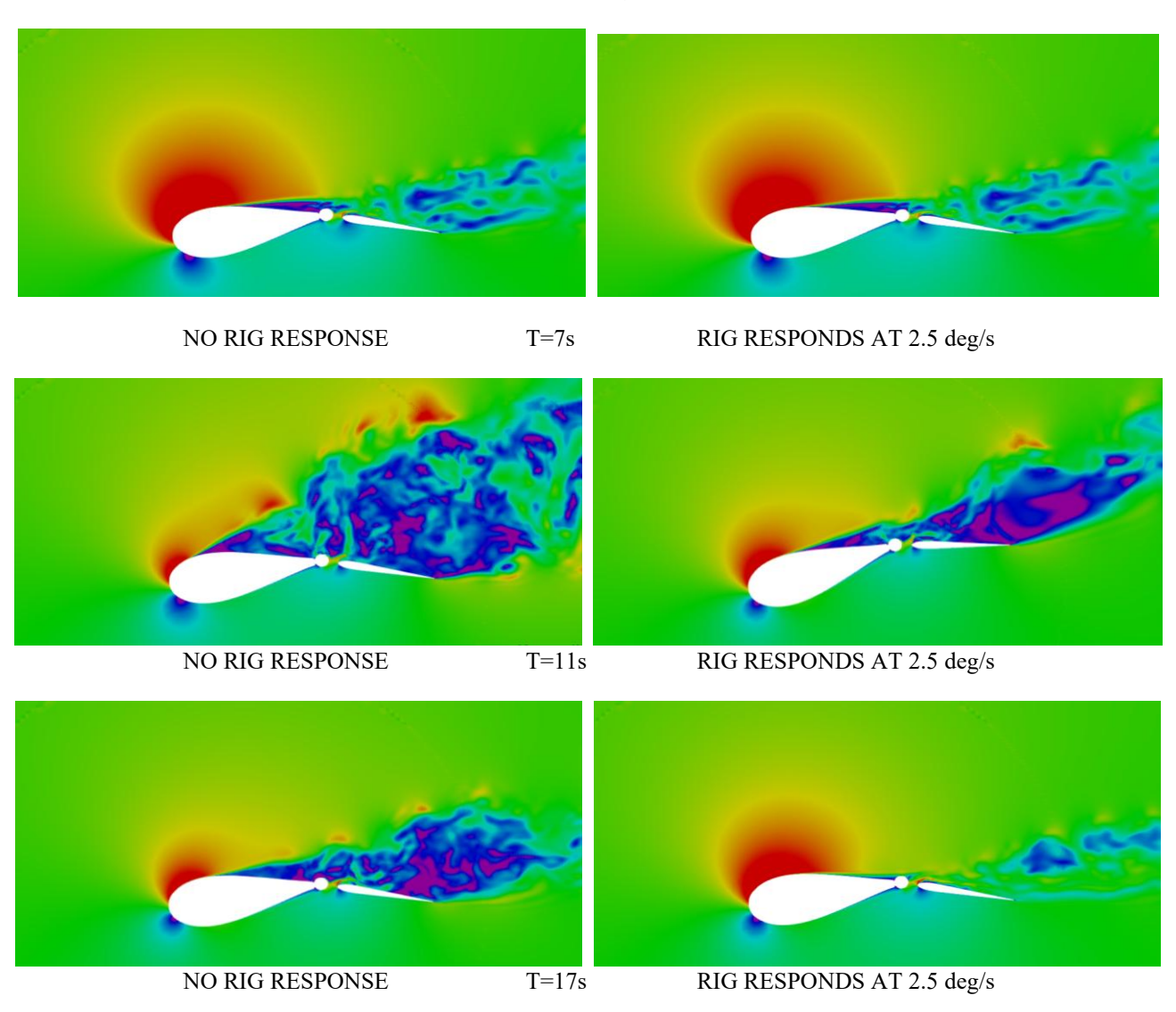


Figure 9 – Visualisation of flow around wing at mid span hinge point for TWA 30°

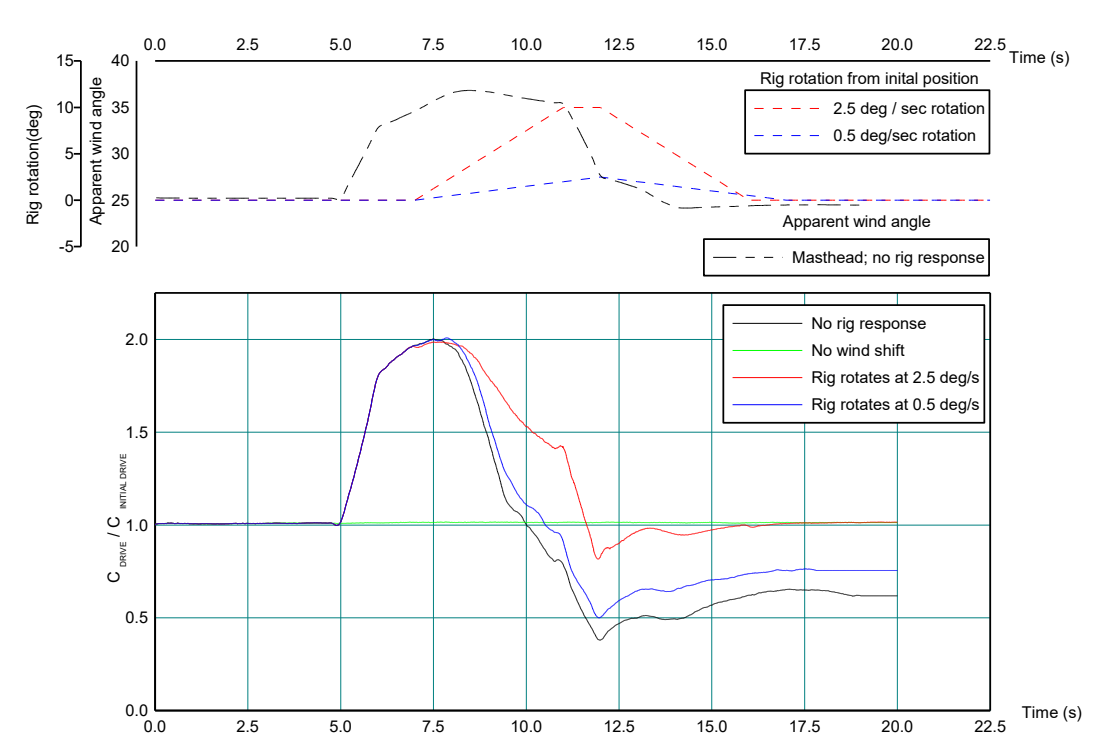


Figure 10 - Drive forces generated by wing for different wing response to wind shift, TWA 30°

8.2 60° TWA CASE

As with the 30° TWA case, forces generated by the wing and velocity and pressure probe points were acquired from the simulations, at the same locations. The resultant forces generated for the different cases modelled are presented in Figure 11. The pressure at four points on the suction side of the wing are presented in Figure 12, with slices throughout the solution shown in Figure 13 for the cases where the wing doesn't respond and responds at $4^{\circ}/s$.

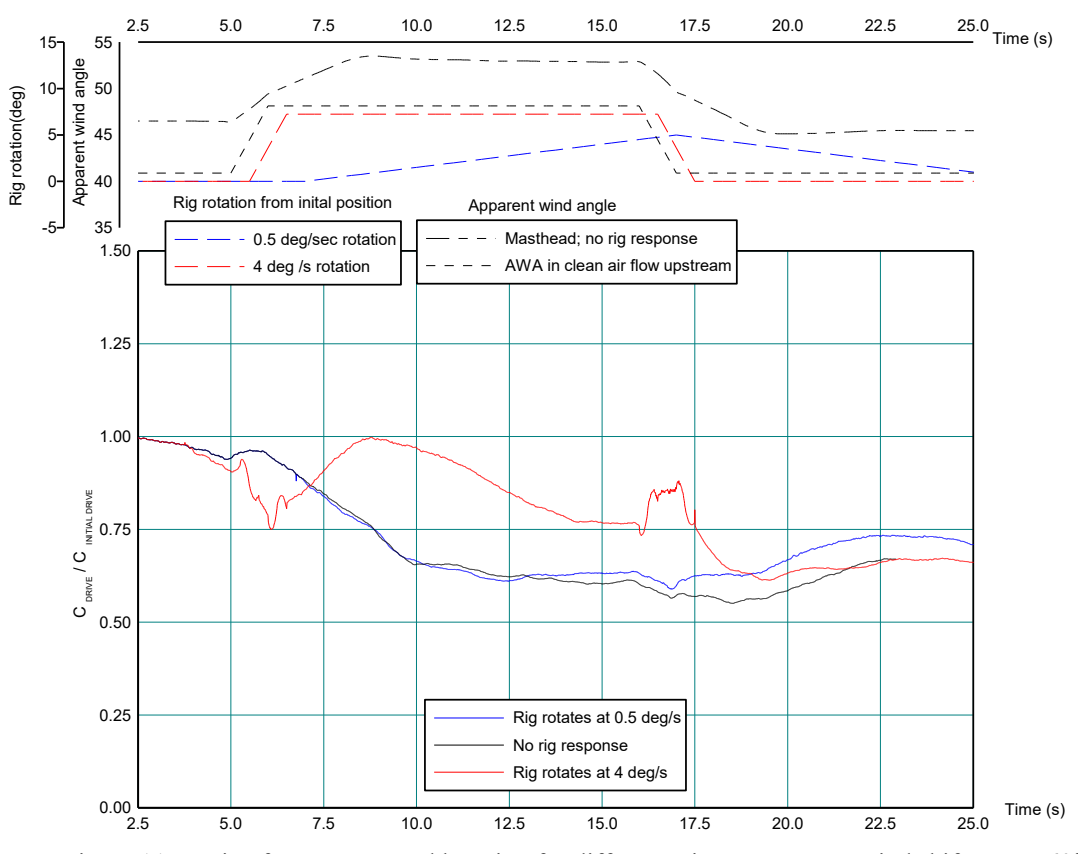


Figure 11 – Drive forces generated by wing for different wing response to wind shift, TWA 60°

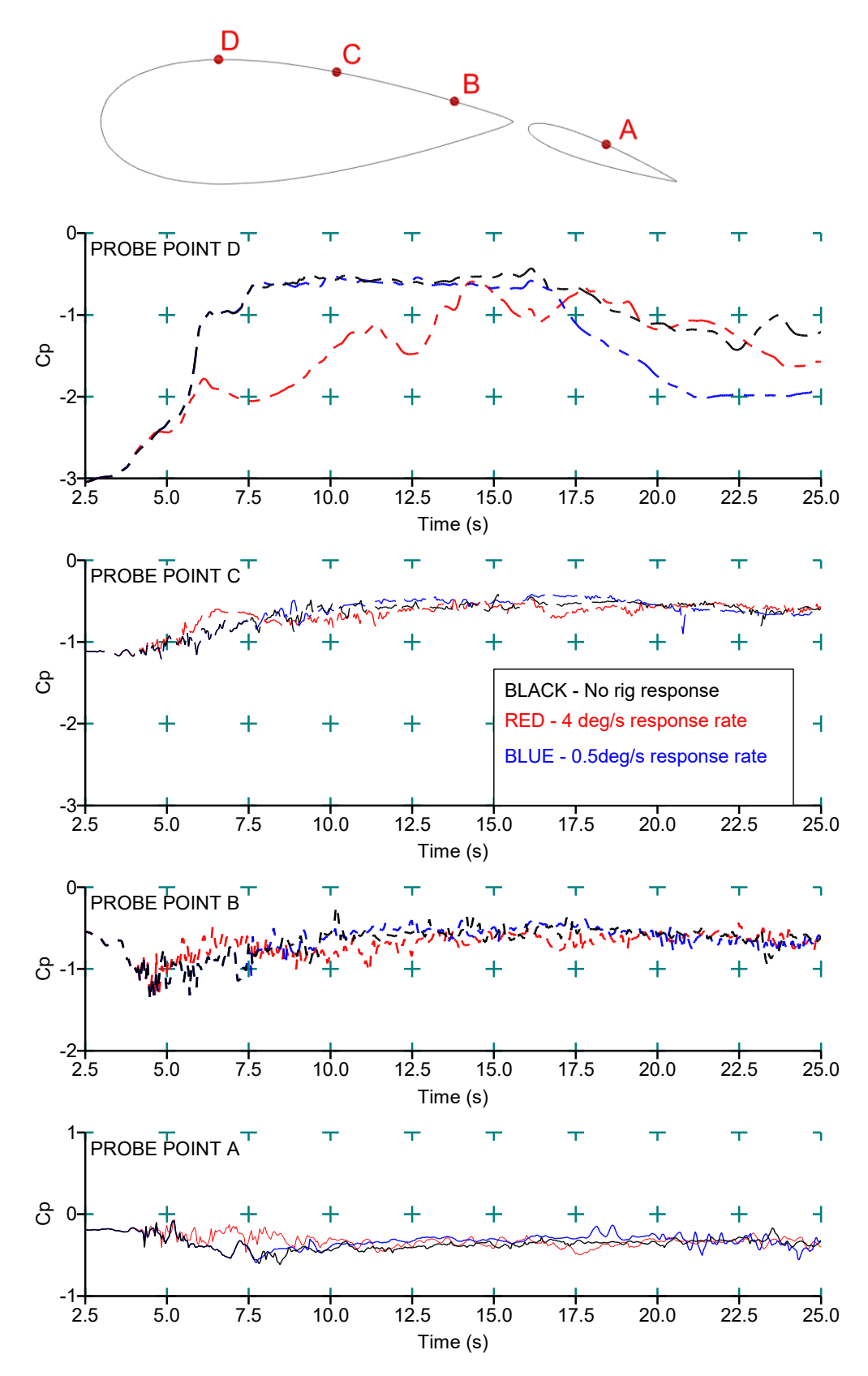


Figure 12 – Pressure coefficients recorded on suction side of wing for different responses to wind shift, TWA 60°

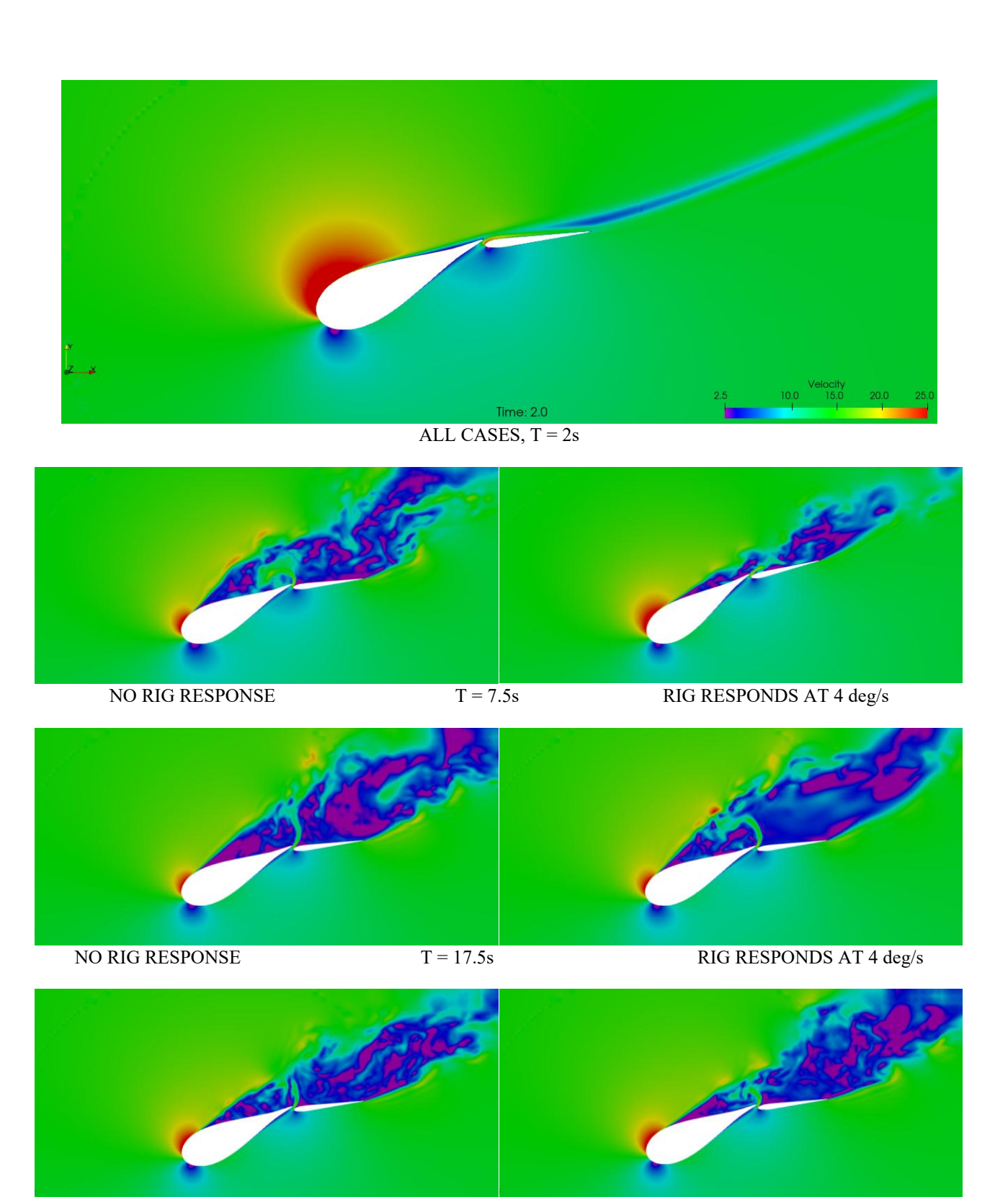


Figure 13 - Visualisation of flow around wing near mid span for TWA 60°

T = 23s

RIG RESPONDS AT 4 deg/s

NO RIG RESPONSE

9. DISCUSSION

Computational fluid dynamics has a proven record of accurately modelling aerodynamic flows such as those described in this paper but, as the verification study in §4 implies, careful selection of turbulence modelling is required when the Reynolds number is in the transition regime, and the use of a free to transition model may give greater correlation with wind tunnel data. This study, and other similar undertakings, have shown also that using unsteady RANS for stalled or near stalled scenarios, as opposed to a steady state RANS simulation is a prudent approach, showing due diligence to time step size. A study of Figure 8 and 10 show changes in pressures and thus forces even after the air velocity has nominally stopped changing, indicating the unsteady nature of stall, and the requirement to model more than just a steady state data point in order to correctly simulate the aerodynamic loading. Aerodynamic stall is unsteady in nature, and hence attempting to model it with a steady state approach inherently neglects some aspects of the underlying physics. The computational requirements of such an approach can be significant; a typical unsteady run of the case study wing took in the order of 7000 core-hours on AMD EPYC 9654, a modern high performance processor, compared to 95 core hours for a steady state solution.

The effect of the wind shift upon the drive force can be observed in Figure 10 and Figure 12 for the two wind angles modelled. In the case of TWA=30, all simulations where the wind shift has occurred show an initial rise in drive as the apparent wind angle and angle of attack increases, as well as the flow being accelerated thus giving further drive beyond that expected for a steady state. The initial case was close to peak drive force for an AWA=20°, but as the wind shifts the AWA increases and the peak drive increases as the target drive force condition shifts from peak efficiency towards peak lift force [5]. For the cases where the wing is not rotated flow separation now occurs (initiating at approximately t=7.5s) with a resultant loss of drive. At this point however the case where the wing is rotated at 2.5°/s shows a much slower decrease in drive force as it manages to maintain some attached flow, and returns to the original loading condition. The effect of not rotating the wing is a decrease in drive even after the wind has returned to the original direction due to the wing remaining in a partially stalled condition. A slow rotation rate of the wing in response to the wind shift can also be seen, for this case, to be insufficient to avoid stall and the resultant long term loss in lift. Such a condition would require further de-loading of the wing to gain fully attached flow before increasing back to peak drive.

For the TWA=60° scenario (Figure 12), the differences due to rate of wing rotation are still clear, but certain characteristics are different from the TWA=30° case. Two points need to be remembered in order to understand the behaviour; as the wind angle changes, the apparent wind speed drops and at these wind angles, the optimum drive force point is closer to stall / peak lift whereas for smaller apparent wind angles the optimum drive force is obtained by maximising the lift to drag ratio. As a result of the drop in wind speed, the drive force drops even though the angle of attack increases and stall has not yet occurred, and because the wing is operating closer to stall than the TWA=30° case any increase in angle of attack is much more likely to induce stall. It can be observed that the fastest rig rotation maintains the suction pressure (Figure 11) initially but there is still a drop in force generated as the wind speed is lower during the wind shift. The lower rate of rig rotation can not avoid stall, and hence peak lift is not regained even after returning to the initial condition. When the wing is rotated back to the original condition at the higher rotation rate it can be observed that the drive force generated drops, the pressure suction peak (probe D, Figure 11) disappears and stall has been induced by the rigs movement rather than the change in wind angle; the rotation rate is too high to maintain attached flow (Figure 13, T=17.5s). It is acknowledge that magnitude of a near instance 10deg wind shift is high and the probability of occurrence is relatively low. This level was selected to explore the feasibility of this unsteady CFD approach

While the maintenance of drive force by rotating the rig at a suitable rate is clear, there are a number of different dynamic effects at play, not just the instantaneous angle of attack. The rotation of the rig can cause acceleration of the air flow, thus momentarily increasing the drive force (a well known and well used technique in small boat sailing [6]), but also can cause the flow to detach if the acceleration is too rapid in the increasing incidence angle direction. The inclusion of inertial effects is important to optimise performance.

Figure 9 and Figure 13 show significant zones of separated flow even when the rig responds quickly, so it is to be expected that a stall control algorithm needs to operate on appropriate time periods, and also that zones of separated flow are to be expected, even for wind angles requiring maximum lift, and thus separated flow should be desired and controlled rather than eliminated completely.

For the case study presented a simple control trigger of a change in the apparent wind angle was used, but the use of surface pressure is a better guide to the actual wing loading, and thus performance. Figure 8 shows the drop in the suction peak (probe point D) and then recovery for the 2.5°/s rotation case and the lack of recovery for the 0.5°/s rotation case. Indicating it needs further rotation to regain attached flow. Use of just the local apparent wind angle (Figure 7) does not provide this information and thus can leave the rig in a poorly performing orientation if and when operating in highly unsteady or unstable wind conditions.

The case study presented in this paper is just two data points in the full performance envelope required to correctly model a solid wing sail, showing an approach towards developing and optimising a control method using a simple trigger to instigate a change in the wing's orientation. There are many different aspects of instigating and controlling the rigs movement not investigated yet, such as pressure probe location, sampling period and averaging, length of period before rig response, and rate of rig response to name a few.

It is clear however from both the wind tunnel testing of Hillenbrand [3] and the CFD modelling presented here that stall hysteresis effects mean full aerodynamic stall should be avoided as it requires a complete de-loading of the wing in order to obtain flow reattachment. This has further implications, depending upon the control algorithm and mechanical response times, as to the maximum loading the rig should be set at in rapidly changing conditions such as a weather front or in the lee of high mountains. The wind angle changes used in this paper are large over the timescales presented, but not unrealistic.

Steady state performance predictions show strong interactions between the rig and the hull form, hence there is further work to undertake in investigating the effect of the hull form upon stall, as well as monitoring and controlling stall behaviour in the arrays of wings expected to be required for larger vessels.

10. CONCLUSIONS

A computational approach to modelling stall of a solid wing sail has been developed using unsteady RANS that shows good correlation with wind tunnel data. The case studies of a full scale design show that partial stall can remain after returning to pre stall angles of attack if the wing is allowed to reach full stall even for relatively small periods of time.

The use of local apparent wind angle without some measure of wing load such as surface pressure or structural load, has been shown to be insufficient to gain optimal performance in a control algorithm in highly variable flow conditions.

There is a range of further work in the topic of designing wind propulsion devices for stall recovery to be undertaken, including wind tunnel testing to allow further verification of the approach, further integration of control algorithms into the computational model and investigation of different control approaches.

11. ACKNOWLEDGEMENTS

This project has been assisted by the UK Innovate "Winds of Change" project, part of the Clean Maritime Demonstration Competition Round 3 (CMDC3) and the authors acknowledge the use of the IRIDIS High Performance Computing Facility in the completion of this work.

We would like to thank Smart Green Shipping for their support in providing design geometry information and support for this project.

12. REFERENCES

- 1 SCHINAS, O. and METZGER, D. "Financing ships with wind assisted propulsion Technologies", RINA Wind Propulsion, London UK, 2019
- 2 CHOU, T., KOSMAS, V., ACCIARO, M. and RENKEN, K., "A Comeback of Wind Power in Shipping: An Economic and Operational Review on the Wind-Assisted Ship Propulsion Technology." Sustainability 13, no. 4 (2021)
- 3 HILLENBRAND, A, GIOVANETTI, L.M., DHOME, U. & KUTTENKEULER, J, "Wind Tunnel tests of a Two-Element Wingsail with focus on Near-Stall Aerodynamics" 8th High Performance Yacht Design Conference March 2024
- FLUCK, M., et al "Progress in development and design of DynaRigs for commercial ships", 24th Chesapeake Sailing Yacht Symposium, March 2022
 - 5 TETTERS, J., RANZENBACH, R. and PRINCE, M., "Changes to Sail Aerodynamics in the IMS Rule", The 16th Chesapeake Sailing Yacht Symposium, March, 2003
- 6. AUBIN, N., DHOME, U., AUGIER, B., BOT, P., Frédéric Hauville. How to be the best at sail pumping?., Jun 2016, Paris, France. pp.5. hal-02141145

13. AUTHORS BIOGRAPHY

Alexander Wright holds the position of Principal Research Engineer at the Wolfson Unit for Marine Technology and Industrial Aerodynamics at the University of Southampton. His primary areas of expertise involve wind tunnel testing, computational modelling and software development. He has conducted CFD modelling of a wide range aerodynamic devices and structures, including offshore racing yachts, Americas Cup solid wingsails and various wind assisted shipping concept designs.

Lloyd Jones holds the position of Senior Research Engineer at the Wolfson Unit for Marine Technology and Industrial Aerodynamics at the University of Southampton. His primary area of expertise is the application of computational fluid dynamics to a wide range of aero and hydrodynamic problems, including performance prediction for ships and yachts, propulsion systems, green shipping and renewable energy technology.

Martyn Prince holds the position of Principal Research Engineer at the Wolfson Unit for Marine Technology and Industrial Aerodynamics at the University of Southampton. His primary areas of expertise involve aerodynamic and hydrodynamic experimental testing and sailing (and wind assisted) vessel performance prediction.